Cancer Research

Myeloid-Derived Suppressor Cell Inhibition of the IFN Response in Tumor-Bearing Mice

Bethany L. Mundy-Bosse[1], Gregory B. Lesinski[2], Alena C. Jaime-Ramirez[1], Kristen Benninger[3], Mahmood Khan[4], Periannan Kuppusamy[2,4], Kristan Guenterberg[3], Sri Vidya Kondadasula[5], Abhik Ray Chaudhury[6], Krista M. La Perle[7], Melanie Kreiner[3], Gregory Young[8], Denis C. Guttridge[9], and William E. Carson, III[3,9]

Abstract

Our group and others have determined that immune effector cells from patients with advanced cancers exhibit reduced activation of IFN signaling pathways. We hypothesized that increases in immune regulatory cells termed myeloid-derived suppressor cells (MDSC) could interfere with the host immune response to tumors by inhibiting immune cell responsiveness to IFNs. The C26 murine adenocarcinoma model was employed to study immune function in advanced malignancy. C26-bearing mice had significantly elevated levels of $GR1^+CD11b^+$ MDSC as compared with control mice, and splenocytes from tumor-bearing mice exhibited reduced phosphorylation of STAT1 (P-STAT1) on Tyr^{701} in response to IFN-α or IFN-γ. This inhibition was seen in splenic $CD4^+$ and $CD8^+$ T cells as well as natural killer cells. *In vitro* coculture experiments revealed that MDSC inhibited the IFN responsiveness of splenocytes from normal mice. Treatment of C26-bearing mice with gemcitabine or an anti-GR1 antibody led to depletion of MDSC and restored splenocyte IFN responsiveness. Spleens from C26-bearing animals displayed elevated levels of iNOS protein and nitric oxide. *In vitro* treatment of splenocytes with a nitric oxide donor led to a decreased STAT1 IFN response. The elevation in nitric oxide in C26-bearing mice was associated with increased levels of nitration on STAT1. Finally, splenocytes from iNOS knockout mice bearing C26 tumors exhibited a significantly elevated IFN response as compared with control C26 tumor-bearing mice. These data suggest that nitric oxide produced by MDSC can lead to reduced IFN responsiveness in immune cells. *Cancer Res; 71(15); 5101–10. ©2011 AACR.*

Introduction

Previous studies showed that the endogenous production of IFN is essential for immunosurveillance against developing tumors (1, 2). It has been determined that mice lacking either the IFN-γ receptor (IFN-γR1) or the major IFN signal transducer STAT1, developed tumors at a faster rate than wild-type mice following exposure to the carcinogen 3-methylcholanthrene (MCA). In addition, mice lacking IFN-γR1 or STAT1 as well as the tumor suppressor p53 developed a wider range of spontaneous tumors as compared with wild-type mice lacking p53 only (1). Studies by Dunn and colleagues have also shown the distinct importance of IFN-α/β sensitivity in cells of the hematopoietic lineage for immunoediting and antitumor immunity *in vivo* (3). IFNs are now accepted as critical mediators of immunosurveillance and are important in both innate and adaptive antitumor immune responses. A functional immune system in patients with cancer is also critical for the success of immune-based therapies, such as exogenously administered cytokines, vaccines, and targeted antibodies via the induction of type I IFNs (e.g., IFN-α, IFN-β) and type II IFNs (IFN-γ). Our group and others have determined that immune effector cells from patients with advanced cancers exhibit reduced activation of IFN-induced signaling pathways (4, 5). One potential mechanism for the immune inhibition seen in tumor-bearing hosts is the presence of increased numbers of immune suppressor cells.

Myeloid-derived suppressor cells (MDSC) are a heterogeneous population of early myeloid cells that accumulate in the blood and tumors of patients with cancer. Their numbers correlate with tumor burden (6). These cells arise from myeloid precursors in response to tumor-derived growth factors and proinflammatory cytokines (6, 7). MDSC are described phenotypically in murine models as $GR1^+CD11b^+$, with subsets expressing IL-4Rα (7, 8). MDSC have been shown to reside in the peripheral blood, lymphoid tissue, and tumor tissue of mice in a number of experimental models (6, 9–13).

Authors' Affiliations: Departments of [1]Integrated Biomedical Sciences, [2]Internal Medicine, and [3]Surgery, [4]The Dorothy M. Davis Heart and Lung Research Institute, [5]Department of Oncology, Karmanos Cancer Institute, [6]Department of Pathology, [7]Department of Veterinary Biosciences, College of Veterinary Medicine, [8]The Center for Biostatistics, and [9]Department of Molecular Virology, Immunology, and Medical Genetics, Arthur G. James Cancer Hospital and Richard J. Solove Research Institute, The Ohio State University, Columbus, Ohio

Note: Supplementary data for this article are available at Cancer Research Online (http://cancerres.aacrjournals.org/).

Corresponding Author: William E. Carson, III, The Ohio State University, N924 Doan Hall, 410 W. 10th Avenue, Columbus, OH 43210. Phone: 614-293-6306; Fax: 614-293-3465; E-mail: william.carson@osumc.edu

doi: 10.1158/0008-5472.CAN-10-2670

Prior studies have shown that MDSC can inhibit the effector function of natural killer (NK) and T cells in tumor-bearing animals through multiple mechanisms, including the release of immune-suppressive cytokines, the generation of nitric oxide and reactive oxygen species, and the depletion of arginine or cystine from the tumor microenvironment (6, 14, 15). Studies in murine models indicate that disruption of MDSC function can reverse immune tolerance to tumor antigens, stimulate antitumor immune responses, and markedly inhibit tumor growth (6, 7).

We hypothesized that elevated numbers of MDSC present in the setting of advanced malignancy would inhibit the response of immune cells to type I and type II IFNs. The results of our experiments showed that mice bearing C26 adenocarcinoma tumors exhibit elevated numbers of MDSC which led to increased nitration on STAT1 and impaired responsiveness of immune effector cells to IFNs.

Methods

Cytokines and reagents

Recombinant murine IL-6 and IFN-γ were purchased from R&D Systems, Inc. Recombinant Universal Type I Interferon (IFN-A/D) was purchased from PBL Biomedical Sciences. S-nitroso-*N*-acetylpenicillamine (SNAP) was purchased from Molecular Probes.

Murine tumor models

Male 4- to 6-week-old BALB/c × DBA/2F$_1$ (CD2F1) mice were used (Harlan). Colon 26 (C26) tumor cells (10^6 cells) were injected subcutaneously into the flank of CD2F1 mice (16). Male Balb/c By and iNOS knockout mice were injected with C26 tumor cells (10^6 cells) for nitric oxide studies (4–6 weeks; Jackson Labs). Female BALB/c mice (4–6 weeks; Harlan) were injected in the mammary fat pad with 5×10^4 4T1 tumor cells.

Intracellular flow cytometry

Levels of P-STAT1 and STAT1 were measured via flow cytometry in cells derived from murine splenocytes or lymph nodes following *in vitro* stimulation with PBS, IFN-A/D, or IFN-γ as described previously (4). Data were expressed as specific fluorescence ($F_{sp} = F_t - F_b$), where F_t represents the median value of total staining and F_b represents the median value of background staining with an isotype control antibody (4, 17, 18). CD4, CD8, and CD49b antibodies were used for surface staining of immune subsets (BD Biosciences). For nitration flow cytometry, splenocytes were colabeled with anti–STAT1-PE and anti–nitrotyrosine-alexafluor-488 antibody (BD Biosciences and Millipore).

Real-time PCR

Following TRIzol extraction (Invitrogen) and RNeasy purification (Qiagen), total RNA was quantitated and reverse transcribed as previously described (19). The resulting cDNA was used to measure gene expression by real-time PCR by using predesigned primer/probe sets and 2× TaqMan Universal PCR Master Mix with 18s rRNA as an internal control (Applied Biosystems).

Immunoblot analysis

Lysates were prepared from splenocytes following *in vitro* stimulation with PBS or IFN-A/D and assayed for the expression of proteins by immunoblot (19). For the detection of nitrated STAT1, samples were immunoprecipitated with STAT1 (BD Biosciences) and then probed with an anti-nitrotyrosine antibody (Invitrogen).

Flow cytometric analysis of myeloid derived suppressor cells

Analysis of the MDSC in splenocytes was conducted as previously described (8). Briefly, 10^6 splenocytes were labeled with fluorochrome-labeled antibody-targeting murine CD11b, GR1, IL-4Rα, or appropriate isotype control antibody (BD Biosciences) for 1 hour at 4°C, washed, resuspended in 1% formalin, and analyzed via flow cytometry.

Immunofluorescent staining of MDSC

Tumors were fixed in 4% paraformaldehyde overnight, dehydrated in sucrose, and embedded in ornithine carbamyl transferase (OCT) and frozen. Frozen sections (5 μm) were probed with anti-GR1 alexafluor 488 (Invitrogen) and anti-CD11b alexafluor 647 (BD Bioscience) antibodies, or appropriate isotype control. Sections were also labeled with 4′,6-diamidino-2-phenylindole (DAPI) nuclear stain. Slides were analyzed on an Olympus FV1000 Spectral Confocal microscope.

Isolation of MDSC from C26-bearing mice

Spleens were harvested aseptically from tumor-bearing mice (18), filtered through 70 μmol/L cell strainers, washed with PBS, and resuspended in media. GR1$^+$CD11b$^+$ MDSC were isolated by using anti-GR1 biotinylated beads (Miltenyi Biotec) with purity greater than 95% by flow cytometry. Isolated MDSC were cocultured with splenocytes at a 1:3 ratio. This ratio recapitulates the number of MDSC present within the spleen of a C26-bearing mouse. After 24 hours, splenocytes were harvested from culture and stimulated with IFN-A/D (10^4 U/mL) for 15 minutes. IFN-induced levels of P□STAT1 were measured by flow cytometry as described.

MDSC depletion with GR1 antibody

On day 20 post-tumor inoculation with C26, mice were treated with either anti-GR1 (BD Biosciences) or isotype control antibody (Sigma) at a concentration of 0.25 mg/mouse in 200 μL PBS. MDSC depletion was verified in the spleen and tumor by flow cytometry and immunofluorescent staining of frozen tumor sections

Gemcitabine treatment of C26-bearing mice

Two days after C26 tumor inoculation, mice received twice weekly intraperitoneal injections of gemcitabine (Gemzar; Eli Lilly) at a dose of 75 μg/g of body weight. This agent has been previously validated as an effective means of reducing MDSC (20–22). For 24 hour depletion studies, mice were injected with 75 μg/g gemcitabine 24 hours prior to animal harvest. MDSC depletion was also verified in the tumor by immunofluorescent staining of frozen tumor sections.

Measurement of nitric oxide by DAF-FM

Spleens were washed with an ice-cold PBS buffer and embedded in OCT. Frozen segments (6 μm) were incubated with 10 μmol/L DAF-FM (4-amino-5-methylamino-2',7'-difluorescein) diacetate (Molecular Probes; D-23842) for 30 minutes at 37°C. The images were obtained by a fluorescence microscope (Nikon), and intensity was quantitatively determined by MetaMorph image analysis software (Molecular Devices).

Immunohistochemistry of tumors

Tumors were fixed in formalin, washed with PBS, paraffin embedded, sectioned into 4-μm slices, attached to lysine-coated slides, and stained with hematoxylin and eosin as previously described (23). Briefly, replicate sections were deparaffinized in xylene, rehydrated, and endogenous peroxidase activity was blocked with 3% hydrogen peroxide for 5 minutes, followed by rinses in diH_2O. Ag retrieval was achieved in Dako's target retrieval solution (Dako S1699) by heating slides at 94°C for 30 minutes and cooling at room temperature for 15 minutes. Slides were then incubated for 60 minutes with antibodies specific for CD34 (Abcam; clone MEC14.7), and Ki67 (Thermo; clone SP6). Detection was achieved with the Vectastain Elite ABC system and Novared Chromogen (Vector). All samples were examined in a blinded fashion by an experienced pathologist (K.M. La Perle), using an Olympus BX45 light microscope with an attached DP25 digital camera (B & B Microscopes Limited). Automatic quantification was carried out on whole slide images scanned at ×40 magnification (ScanScope XT; Aperio Technologies), using the Positive Pixel Count Algorithm in the ImageScope software (Aperio Technologies).

Statistical analysis

Two-sample *t* tests were used to compare outcomes (e.g., IL-6, Ifit2, P-STAT1) between groups. If necessary, outcomes were log transformed to meet the assumptions of normality and constant variance for the test. Pearson correlation coefficients were used to quantify the relationship between outcomes. Tumor growth was assumed to be log linear and a mixed effects model with a random intercept and slope for each animal was used to estimate the rate of increase. *P* values less than 0.05 were considered statistically significant.

Results

Decreased IFN response of immune cells from tumor-bearing mice

We hypothesized that immune effector cells in tumor-bearing mice would have an altered response to cytokines that promote antitumor immunity as is seen in patients with advanced malignancy. Of particular interest were the type I and type II IFNs, as these cytokines mediate tumor immunosurveillance, and reductions in immune cell IFN responsiveness have been shown to exist in cancer patients (1–3, 24). The C26 model was chosen for this study because of its rapid tumor growth and ability to mimic advanced clinical disease. The ability of IFN-α or IFN-γ to activate the STAT1 transcription factor (by phosphorylation at Tyr^{701}) was measured by intracellular flow cytometry in splenocytes from normal and C26-bearing mice (Fig. 1; representative histogram in Supplementary Fig. S1A). Induction of P-STAT1 following a 15 minute

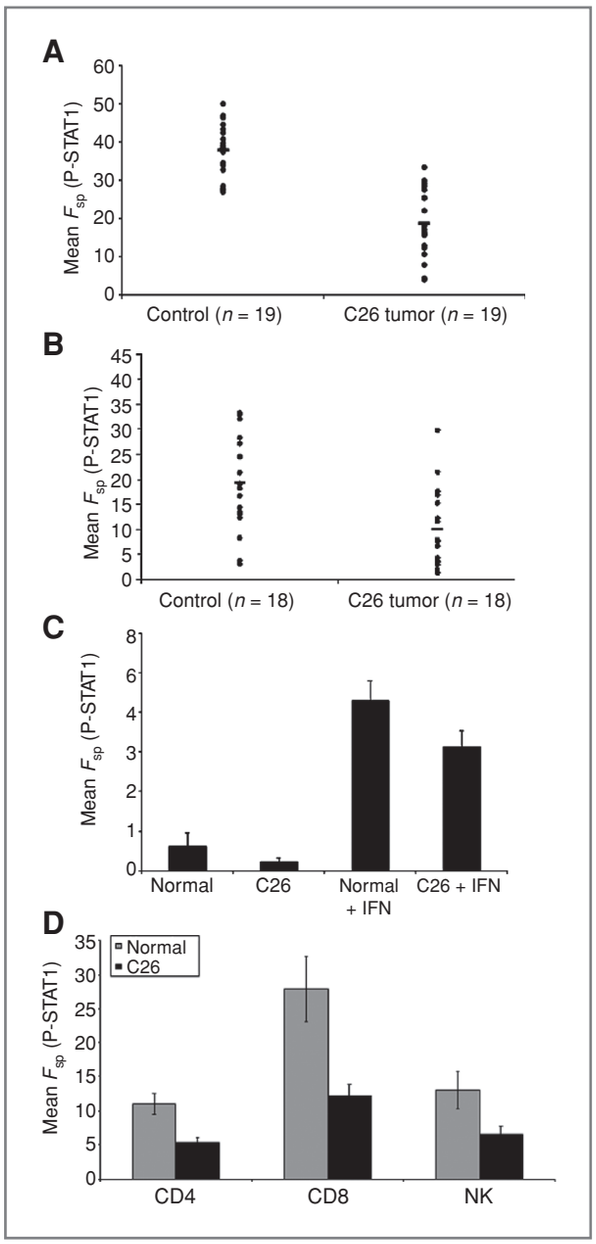

Figure 1. Decreased IFN response in tumor-bearing mice. P-STAT1 was measured in splenocytes from control (Control) or day 22 C26 tumor-bearing mice (C26 tumor) by intracellular flow cytometry following stimulation with IFN-α (10^4 U/mL; A) or IFN-γ (10 ng/mL; B). *Y*-axis is specific fluorescence (F_{sp}) of staining for P-STAT1. C, P-STAT1 was measured in splenocytes from untreated normal mice and mice bearing C26 tumors, or from mice stimulated with 2×10^4 U IFN-A/D *in vivo* and harvested 2 hours later. D, P-STAT1 was measured following IFN stimulation in splenocytes that were colabeled with antibodies against CD4, CD8, and CD49b (NK).

stimulation of splenocytes with IFN-A/D (10^4 U/mL) was significantly reduced at day 22 in C26-bearing mice [mean fluorescence intensity (MFI) of P-STAT1 = 18.8; range = 4.0–33.4] as compared with control mice (MFI of P-STAT1 = 37.9; range = 27.0–50.0; Fig. 1A; $P < 0.0001$). Induction of P-STAT1 was also significantly decreased in splenocytes from C26-bearing mice following stimulation with 10 ng/mL IFN-γ (Fig. 1B; $P = 0.003$). MDSC (approximately 15%–20% of total splenocytes) were excluded from this analysis by gating to ensure that the lymphocyte populations of normal and tumor-bearing animals were of comparable composition. These results were validated by immunoblot analysis (Supplementary Fig. S1B). The decrease in IFN responsiveness was also observed in cells derived from lymph nodes (Supplementary Fig. S1C). To evaluate the effect of the C26 tumor on IFN on responsiveness *in vivo*, normal or C26 tumor-bearing animals were injected with IFN-A/D (2×10^4 U) and splenocytes were harvested 2 hours later for analysis. The level of P-STAT1 was evaluated by intracellular flow cytometry as described previously (Fig. 1C). As expected, the P-STAT1 response was reduced in mice bearing C26 tumor both at baseline and in response to exogenous administration of IFN. An analysis of IFN responsiveness in lymphocyte subsets by dual parameter intracellular flow cytometry revealed that the induction of P-STAT1 was inhibited in CD4, CD8, and CD49b (NK cells; Fig. 1D; CD4, $P = 0.009$; CD8, $P = 0.002$; NK, $P = 0.02$). We next analyzed the induction of the IFN-α-stimulated gene interferon-induced protein with tetratricopeptide repeats 2 (*IFIT2*) and the IFN-γ-stimulated gene IFN regulatory factor 1 (*IRF1*) by quantitative real-time PCR following a 4 hour *in vitro* treatment of splenocytes from C26 bearing or normal mice with either IFN-A/D (10^2 U/mL or 10^4 U/mL) or IFN-γ (10 ng/mL). The expression of *Ifit2* was significantly reduced in splenocytes obtained from C26-bearing mice as compared with controls ($n = 5$ mice per group) at both doses of IFN-A/D (normal = 92.7 ± 24.5 vs. C26 36.4 ± 12.6, $P = 0.0018$ at 10^2 U/mL; normal = 202.2 ± 21.7 vs. C26 99.9 ± 17.2, $P = 0.0059$ at 10^4 U/mL; Fig. 2A). The expression of *Irf1* was also significantly reduced in splenocytes from C26-bearing mice ($n = 5$–6 mice per group) versus controls following a 4-hour stimulation with IFN-γ (Fig. 2B; $P < 0.05$). We also evaluated expression of the IFN-inducible genes *ISG15*, *OAS1*, and *IRF8* and observed similar trends (Supplementary Fig. S3A and B; data not shown).

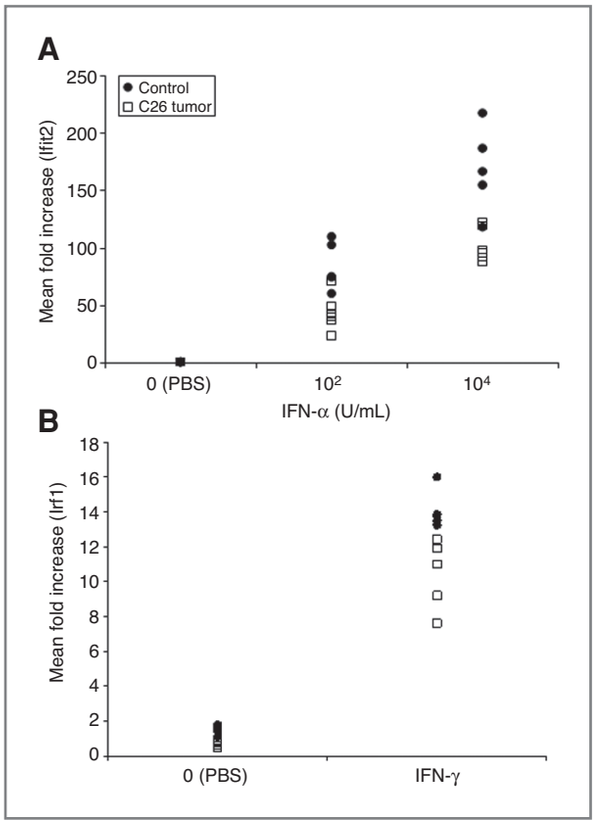

Figure 2. Attenuated IFN-stimulated gene expression in splenocytes from C26-bearing mice. A, total RNA was isolated from splenocytes of control or mice bearing C26 tumor following stimulation of the cells for 4 hours with IFN-A/D or PBS, converted to cDNA and analyzed by real-time PCR for *Ifit2*. B, *Irf1* expression was evaluated in a similar manner following stimulation of splenocytes with PBS or IFN-γ (10 ng/mL). Real-time PCR data were obtained in triplicate and are expressed as the mean fold increase relative to the level of 18s mRNA. Each symbol represents the fold change of an individual animal.

MDSC levels are elevated in tumor-bearing mice, and are associated with decreased IFN response *in vitro*

Flow cytometric analysis showed a significantly higher percentage of MDSC in splenocytes from C26-bearing mice as compared with splenocytes from control animals (Fig. 3A and B; ref. 25). Histologic analysis of splenic tissue revealed extramedullary hematopoiesis and abundant myeloid precursors resulting in extensive splenomegaly (data not shown). Time course studies revealed that an increase in MDSC occurred as early as 7 days post-tumor inoculation (Supplementary Fig. S2A). To test whether MDSC can directly inhibit IFN responsiveness of immune cells, a series of *in vitro* studies was initiated in which $GR1^+CD11b^+$ MDSC were isolated from splenocytes of C26-bearing mice and cocultured with immune cells from tumor-naive animals. Splenocytes isolated from normal mice and cocultured with MDSC had a reduced level of IFN-stimulated P-STAT1 as compared with normal splenocytes cultured for the same time period (Fig. 3C; MFI of P-STAT1 = 22.87 vs. 33.61; $P = 0.0004$). P-STAT1 was measured in the lymphocyte population only, excluding MDSC from analysis by gating. We also showed that elevated MDSC levels were associated with concomitant decreases in IFN responsiveness in the 4T1 murine epithelial cancer model (Supplementary Fig. S2B) which supported the association of MDSC with reduced generation of P-STAT1 in response to IFN-α.

Reduction of MDSC leads to restored IFN responsiveness in C26-bearing mice

C26-bearing animals were treated with the drug gemcitabine, a nucleoside analog, which has been previously employed by other groups to deplete MDSC (20–22, 26). This treatment regimen led to a decrease in the percentage of MDSC present within splenic tissues (Fig. 4A; 10.1% vs. 3.7%; $P = 0.0010$). We also treated mice with a single dose of

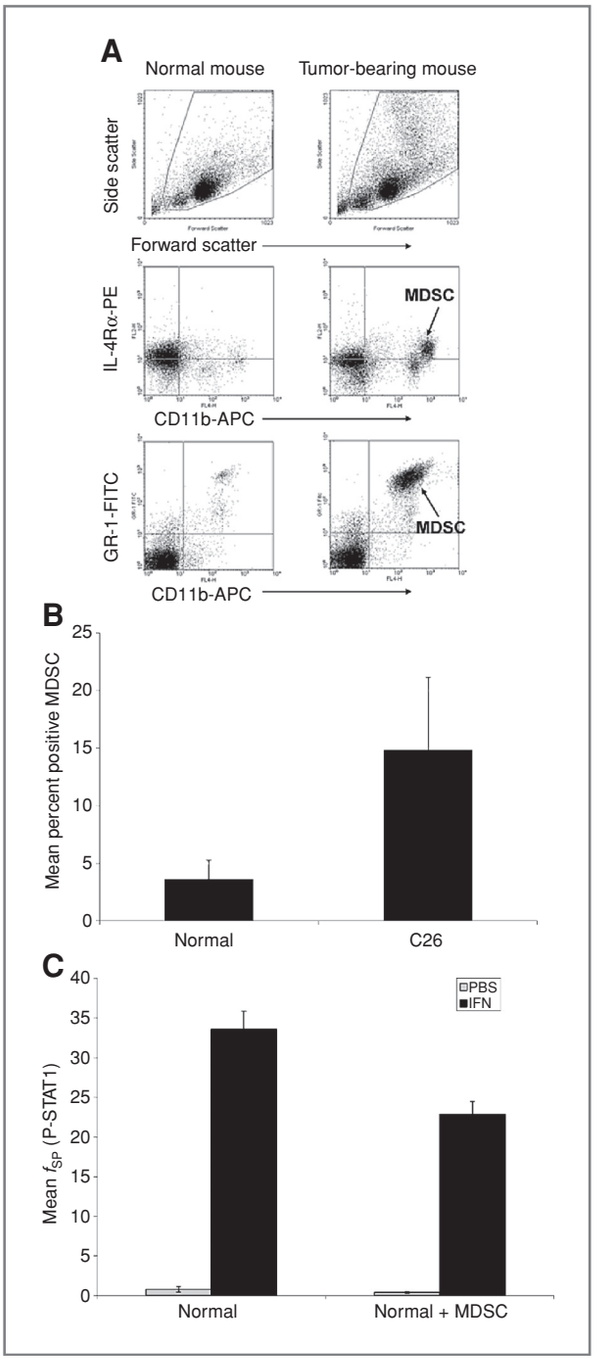

Figure 3. MDSC are elevated in tumor-bearing mice and are associated with decreased IFN responsiveness *in vitro*. A, splenocytes from day 22 C26 mice were evaluated for MDSC by using antibodies targeting GR1, IL-4Rα, and CD11b. B, splenocytes from day 22 C26 mice were evaluated for MDSC by using antibodies targeting GR1 and CD11b. MDSC percentage in splenocytes from day 22 C26 tumor-bearing mice (C26; $n = 19$) or controls (Normal; $n = 22$) as described above. C, MDSC were isolated from C26 splenocytes by magnetic labeling with anti-GR1 beads. After 24 hours, P-STAT1 was measured in splenocytes obtained from control mice ($n = 10$) or normal splenocytes that had been cocultured with MDSC at a 1:3 ratio ($n = 10$).

gemcitabine 24 hours prior to spleen harvest, and saw comparable levels of MDSC depletion in splenocytes from C26 tumor-bearing animals. As predicted, long-term gemcitabine treatment reduced tumor growth by approximately 90%, whereas the 24-hour treatment resulted in no change in tumor volume. Splenocytes obtained from C26-bearing mice treated both for long term and for 24 hours with gemcitabine exhibited a restoration of IFN responsiveness as measured by intracellular P-STAT1 flow cytometry and Western blot analysis (Fig. 4B; Supplementary Fig. S4). Notably, when we evaluated the effects of gemcitabine directly on C26 tumor cells *in vitro,* only 15% of C26 cells were apoptotic when using an equivalent dose of gemcitabine (data not shown). C26-bearing animals were also treated with an anti-GR1 antibody 24 hours prior to spleen harvest (day 20 post-tumor inoculation). This short-term depletion strategy was utilized to evaluate the direct effects of MDSC on IFN response in the presence of fully developed tumors. The reduction in MDSC levels (77% decrease) was verified by flow cytometry (Fig. 4C). Splenocytes from tumor-bearing mice treated with one dose of anti-GR1 exhibited a significantly higher IFN response compared with the splenocytes of tumor-bearing mice treated with isotype control as evaluated by intracellular P-STAT1 flow cytometry and Western blot analysis (Fig. 4D, 42% increase in MFI of P-STAT1 at 10^4 U/mL $P = 0.002$; Supplementary Fig. S4). $GR1^+CD11b^+$ MDSC were also evaluated in the tumor after treatment with gemcitabine or anti-GR1. All treatments led to a reduction in intra-tumor MDSC as compared with tumor-bearing control animals (Supplementary Fig. S5).

Elevated nitric oxide and IFN responsiveness

We hypothesized that soluble factors produced from the abundant MDSC present in the splenic tissue could contribute to the reduced IFN response in tumor-bearing mice. We evaluated two of the major mechanisms through which MDSC are known to exert their suppressive effects, and discovered that while arginase I transcript levels were not significantly different in tumor-bearing splenocytes as compared with splenocytes from normal mice, iNOS mRNA levels were dramatically elevated (data not shown; Supplementary Fig. S3C). DAF-FM and iNOS staining and fluorescent microscopic analysis were employed to test whether decreased IFN responsiveness might be associated with increased levels of nitric oxide in the splenic tissue. These data confirmed a dramatic increase in the level of iNOS protein and nitric oxide in splenocytes from C26-bearing mice as compared with spleens from control animals (Fig. 5A). Pretreatment of splenocytes from normal mice with the nitric oxide donor SNAP (Molecular Probes) led to a decreased phosphorylation of STAT1 in response to IFN-α stimulation (Fig. 5B; MFI of P-STAT1 = 35.7 vs. 16.4). STAT1 was immunoprecipitated from equal numbers of splenocytes from normal and C26 tumor-bearing mice and probed with an anti-nitrotyrosine antibody to detect nitration of STAT1 protein. We carried out a Student's *t* test analysis on the densitometry results and determined that the ratio of nitrated STAT1 to total STAT1 in tumor-bearing mice is statistically higher than that in normal mice, showing that C26-bearing animals exhibited significantly elevated nitration

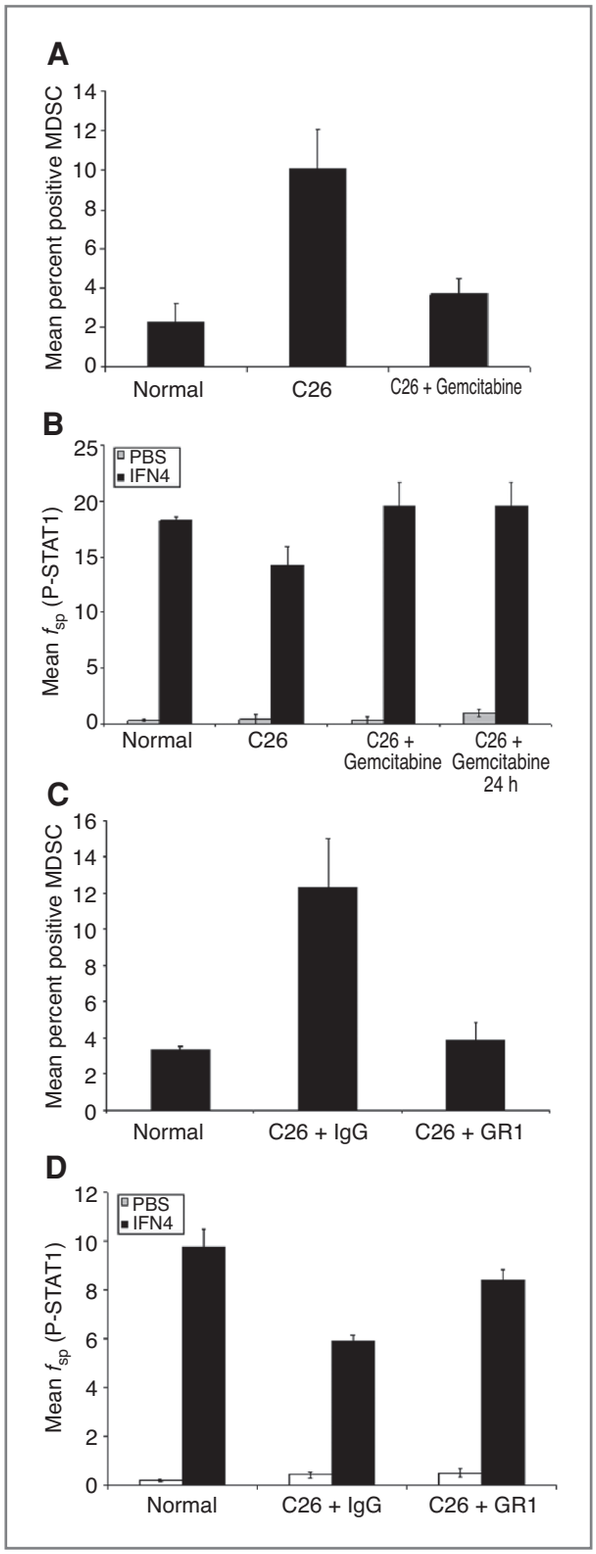

Figure 4. Reduction in MDSC with gemcitabine or anti-GR1 restores IFN responsiveness. A, splenocytes obtained from day 22 C26 tumor-bearing were evaluated by flow cytometry for the presence of MDSC. B, P-STAT1 was measured in splenocytes obtained from control mice (Normal; $n = 5$), day 22 mice bearing C26 tumors and treated with PBS (C26; $n = 5$), day 22 mice bearing C26 tumors and treated with gemcitabine (C26 + gemcitabine; $n = 6$), and day 22 mice bearing C26 tumors and treated with gemcitabine 24 hours prior to harvest (C26 + gemcitabine 24 h; $n = 5$) by intracellular flow cytometry following stimulation with IFN-A/D (10^4 U/mL). C, splenocytes obtained from day 21 control mice (Normal), mice bearing C26 tumors and treated with isotype control (C26 + IgG; $n = 6$), or mice bearing C26 tumors and treated with anti-GR1 (C26 + GR1; $n = 7$) were evaluated for MDSC by flow cytometry. D, P-STAT1 was measured in splenocytes obtained from normal or day 21 tumor-bearing mice and treated with isotype control (C26 + IgG; $n = 6$), or mice bearing C26 tumors and treated with anti-GR1 (C26 + GR1; $n = 7$) by intracellular flow cytometry following a 15-minute stimulation with IFN-A/D (10^4 U/mL).

of STAT1 as compared with control mice ($P = 0.03$; Fig. 5C). In addition, we validated the level of nitrated tyrosine on STAT1 by flow cytometry. Splenocytes from normal and C26 tumor-bearing mice were labeled with antibodies against total STAT1 and nitrotyrosine. Splenocytes from tumor-bearing and normal mice had equal levels of total STAT1. There was significantly more nitrated STAT1 in splenocytes from tumor-bearing animals as compared with splenoctyes from normal mice ($36 \pm 2.0\%$ vs. $17 \pm 0.3\%$; $P < 0.001$; Supplementary Fig. S3D). This result provides direct evidence that nitration on STAT1 was enhanced in C26-bearing mice. These data support a role for nitric oxide in dampening the response of immune effector cells to stimulation with IFN in tumor-bearing animals. To determine the role of nitric oxide in IFN responsiveness *in vivo*, iNOS knockout mice were inoculated with C26 tumor cells and tumors were allowed to grow for 21 days. At the end of the study, tumor sizes were comparable between iNOS knockout mice and wild-type control mice bearing C26 tumors. Splenocytes from iNOS knockout mice exhibited a significantly elevated induction of P-STAT1 in response to IFN stimulation as compared with immune cells from wild-type mice (IFN 10^4 U/mL, $P = 0.01$; Fig. 5D). Quantitative histologic analysis of iNOS-deficient tumors and tumors from wild-type mice revealed a significant decrease in Ki67 staining ($34.24 \pm 0.4\%$ vs. $11.2 \pm 2.85\%$; $P = 0.01$) as well as CD34 expression ($29.93 \pm 2.25\%$ vs. $6.55 \pm 2.77\%$; $P = 0.02$) in iNOS-deficient mice, indicating a reduced proliferation rate as well as decreased vascularity (Fig. 6).

Discussion

In this report, we have shown that immune cells from tumor-bearing mice display a significantly reduced capacity for IFN-induced signal transduction and gene induction via the STAT1 pathway. This inhibitory effect was observed in $CD8^+$ and $CD4^+$ T cells, as well as in NK cells and occurred following both *in vivo* and *ex vivo* IFN stimulation. C26 tumor-bearing mice exhibited enlarged spleens as compared with normal controls and displayed a concomitant increase in the level of $GR1^+CD11b^+$ MDSC, and depletion of MDSC in tumor-bearing mice led to a restoration of IFN responsiveness in immune cells. Consistent with these observations, *in vitro* coculture of splenocytes with MDSC reduced their ability to respond to IFNs. Splenocytes from C26-bearing mice had elevated levels of iNOS protein, nitric oxide production, and STAT1 tyrosine nitration. Importantly, splenocytes from iNOS-deficient mice

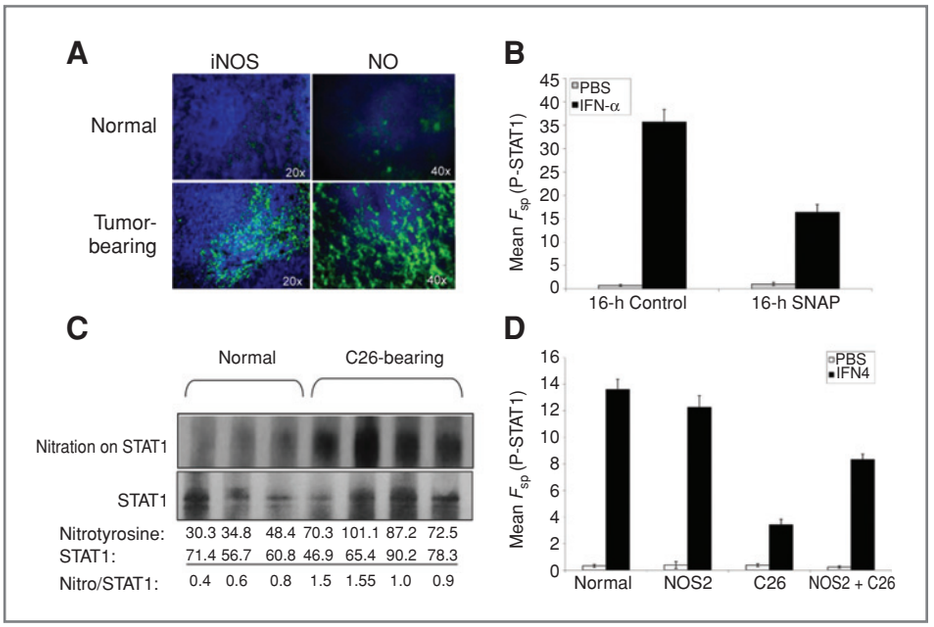

Figure 5. Elevated levels of nitric oxide in tumor-bearing mice inhibits IFN responsiveness in immune cells. A, immunofluorescent staining for iNOS protein (Fitc) and DAPI nuclear counterstain (left); DAF-FM Fitc staining for nitric oxide (NO) and DAPI nuclear counterstain (right). B, splenocytes from normal mice were pretreated with the nitrogen donor SNAP for 16 hours, stimulated for 15 minutes with PBS or IFN-A/D (10^4 U/mL) and evaluated for P-STAT1 by flow cytometry. C, protein lysates from splenocytes of normal or C26-bearing mice were immunoprecipitated with STAT1 antibody and then probed for nitrotyrosine. Lysates were also run on a separate gel and probed with an anti-STAT1 antibody (bottom). Numbers represent densitometry values for nitrotyrosine and STAT1, and the ratio of nitrotyrosine/STAT1 ($P = 0.03$). D, P-STAT1 was measured in splenocytes obtained from day 21 iNOS knockout and control mice with and without C26 tumors by intracellular flow cytometry following stimulation with IFN-A/D (10^4 U/mL).

exhibited improved IFN responsiveness as compared with splenocytes from tumor-bearing wild-type mice. These results indicate that MDSC contribute to the blunted responsiveness of immune cells to IFN-α and IFN-γ via their ability to produce reactive nitrogen species, which leads to reduced IFN-induced signal transduction in immune cells.

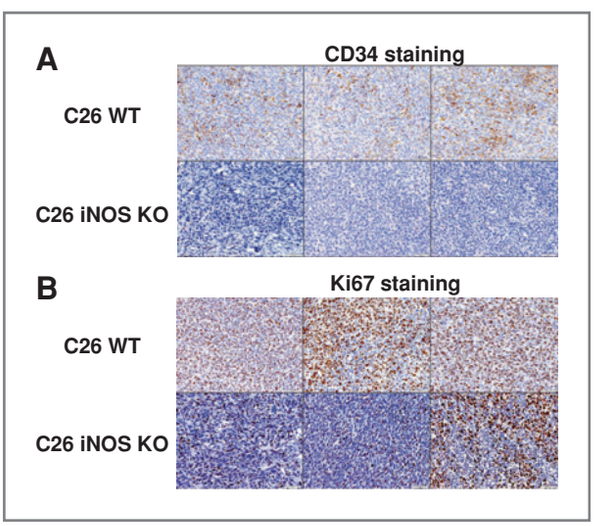

Figure 6. Reduced CD34 and Ki67 expression in tumors from iNOS knockout (KO) mice. Formalin-fixed, paraffin-embedded tumor tissue from C26 tumors in wild-type (WT) mice as compared with iNOS KO mice. Each panel represents an individual mouse tumor section stained with CD34, a vascular endothelial marker ($P = 0.02$; A), or Ki67, a proliferative marker ($P = 0.01$; B).

Our group and others have determined that immune cells from patients with advanced cancers exhibit reduced activation of IFN-induced signaling pathways, although the mechanisms underlying this observation are still under investigation. We utilized the C26 model to recapitulate the complex interactions that take place between immune cells and cancer cells *in vivo*. The IFN response of lymphocytes from C26 tumor-bearing mice (as measured by STAT1 phosphorylation and regulation of IFN-stimulated genes) was significantly reduced when compared with normal mice. It was also noted that the spleens of these mice were enlarged and filled with myeloid precursor cells. Phenotypic characterization revealed that these precursor cells were MDSC, and we hypothesized that they were responsible for the reduced activation of STAT1 in response to IFN-α. Previous work by Mazzoni and colleagues showed that coculture of immortalized murine MDSC with T cells in an *in vitro* nontumor model led to an inhibition of the T-cell response to IL-2 (27). We subsequently showed that the presence of primary MDSC in tumor-bearing animals was associated with altered IFN signal transduction and that removal of this cell population led to restoration of IFN responsiveness. Thus, MDSC seem to be an important regulator of the downstream response to IFNs in tumor-bearing mice. This is the first report in which MDSC have been implicated as a mechanism for the reduced activation of immune cells following IFN stimulation.

Although other tumor or MDSC-derived factors may contribute to reduced IFN responsiveness, our data suggest that the production of nitric oxide by MDSC is a major mechanism in this model. Increased levels of iNOS and nitric oxide in the spleen lead to the nitration of STAT1 on immune cells, which is the proposed mechanism of inhibition of IFN signaling. Importantly, splenocytes from iNOS-deficient tumor-bearing mice had a significantly improved IFN response as compared with splenocytes from wild-type tumor-bearing mice. This finding provides a direct *in vivo* link between excess nitric oxide and decreased IFN responsiveness in the setting of malignancy. In support of these observations, Brito and colleagues (28) have shown that peroxynitrite treatment of peripheral blood mononuclear cells led to increased nitration of tyrosine residues, which inhibited transcription factor phosphorylation following CD3 stimulation, whereas Llovera and colleagues (29) showed that LPS-treated macrophages had an impaired *in vitro* immune cell response to IFN-γ due to an increase in nitric oxide in the culture. We observed that tumor-bearing mice exhibited elevated splenic levels of iNOS protein and treatment of normal splenocytes with SNAP, a nitric oxide donor, suppressed the P-STAT1 response of the splenocytes to IFN-α stimulation. Nitration on STAT1 in primary lymphocytes from tumor-bearing mice has not been shown previously in an *in vivo* murine model. These findings support a role for nitric oxide in the inhibition of IFN signal transduction.

In the studies with iNOS-deficient mice, IFN responsiveness in splenocytes from tumor-bearing animals was not fully restored to levels observed in normal animals. This indicates that other mechanisms may exert an effect on the IFN response in the tumor microenvironment. We evaluated alternative mechanisms that could lead to this inhibition, such as increased levels of arginase I or IL-6. Upregulation of arginase I has been identified as a mechanism of immune suppression that is employed by MDSC (30–32). Although previous studies in macrophages have shown an inverse relationship between iNOS and arginase I levels, it has been shown that in a tumor setting it is possible for iNOS and arginase I to be coexpressed (8, 20, 33, 34). However, splenic levels of this enzyme were not significantly elevated in the C26 model. Although arginase could still play a role in the tumor environment, our data in iNOS-deficient mice suggest that iNOS is a driving factor for the decreased IFN response in immune cells in this model. Despite the observation that immune cells from iNOS-deficient mice exhibited improved responsiveness to IFN, it is important to note that C26 tumors from these knockout mice were similar in size to those from control mice. We anticipated that enhancement of the immune cell IFN response might lead to improved growth control of tumor cells in iNOS-deficient mice and reduced overall tumor volume. However, there was no significant reduction in external tumor size at the end of the study. It is important to note that in this model, the nitric oxide deficiency was present in all host tissues, rather than just the MDSC compartment, and nitric oxide has effects on multiple biologic processes (tumor cell invasion/proliferation, and angiogenesis). A careful quantitative histologic analysis of tumors revealed significantly decreased levels of Ki67 (proliferative marker) and CD34 (expressed on vascular endothelium) in iNOS-deficient mice as compared with those from wild-type mice (Fig. 6). These findings indicate that the iNOS deficiency resulted in biological differences at the site of the tumor. Additional studies would be needed to directly assess the long-term impact of improved IFN response and iNOS-deficiency on survival and antitumor immunity.

The presence of tumor can also induce elevations in proinflammatory cytokines that have been associated with MDSC generation or function. In the C26 model, IL-6 levels were elevated in tumor-bearing mice as compared with normal mice. However, *in vitro* treatment of splenocytes with IL-6 did not alter the P-STAT1 response to IFN-α and administration of exogenous IL-6 was similarly incapable of inhibiting the splenocyte response to this cytokine (Supplementary Fig. S6). Another potential explanation for our results relates to possible changes in levels of Jak-STAT signaling intermediates. However, a careful analysis revealed no significant difference in the protein expression of STAT1, IFN-AR, or Jak1 in splenocytes obtained from tumor-bearing mice as compared with normal control mice (data not shown). As seen in Figure 5C, there was some variability in total STAT1 protein between individual mice, but this variability was not associated with the presence or absence of tumor. Previous work by Brito and colleagues showed that increased nitric oxide did not lead to changes in total STAT1 levels in immune cells, and this was confirmed in the present model when it was shown that STAT1 protein levels were similar in splenocytes from normal and tumor-bearing mice despite high levels of nitric oxide (28).

The observation of decreased IFN responsiveness in immune cells has important implications for the clinical course of disease in cancer patients. Type I and II IFNs play a critical role in mediating the response to immune-based therapies (24). Therefore, conditions that inhibit IFN-induced signal transduction and gene transcription are likely to dampen the responsiveness of the host immune system to immune-based treatments and the host's ability to recognize and eliminate established tumors (35–39). Reports have also shown that type I and II IFNs are functionally important in mediating tumor immunosurveillance against MCA-induced sarcomas and the progression of tumors in p53 null mice (1, 2). Previous studies from our group and others have shown that lymphocytes from patients with metastatic melanoma and other solid malignancies have an inherent reduction in basal and/or IFN-induced STAT1 phosphorylation as compared with normal donors (4, 5, 40). It is important to note that these studies focused on the IFN response in T cells and NK cells, but did not evaluate the responsiveness of dendritic cells or other cell subsets that have been previously shown to play a role in IFN mediated antitumor immunity. These subsets could potentially be impaired by nitrated residues as was observed in other lymphocyte populations. Reduced immune surveillance resulting from nitric oxide–dependent inactivation may therefore be important in the process of tumorigenesis and/or tumor progression.

To our knowledge this is the first *in vivo* report to show that elevated numbers of MDSC are associated with a decreased

cellular response to IFN stimulation in the setting of cancer. Further experiments suggest that increased nitration of STAT1 on tyrosine residues is responsible for the diminished IFN response in splenocytes. Therefore, therapeutic strategies targeted at reducing MDSC or upstream factors could potentially serve to restore IFN responsiveness in tumor-bearing hosts.

Disclosure of Potential Conflicts of Interest

No potential conflicts of interest were disclosed.

Grant Support

This study was supported by the Valvano Foundation for Cancer Research Award (to G.B. Lesinski), and NIH grants CA84402, K24-CA93670 (to W.E. Carson), P01 CA95426 (M. Caligiuri), P30 CA134551 (to M. Caligiuri), K22 CA134551 (to G.B. Lesinski), T32 GM068412 (to B. Mundy-Bosse), T32 GM068412 (to A. Jaime-Ramirez), and T32 CA009338 (to K. Guenterberg).

The costs of publication of this article were defrayed in part by the payment of page charges. This article must therefore be hereby marked *advertisement* in accordance with 18 U.S.C. Section 1734 solely to indicate this fact.

Received July 22, 2010; revised June 8, 2011; accepted June 12, 2011; published OnlineFirst June 16, 2011.

References

1. Kaplan DH, Shankaran V, Dighe AS, Stockert E, Aguet M, Old LJ, et al. Demonstration of an interferon gamma-dependent tumor surveillance system in immunocompetent mice. Proc Natl Acad Sci U S A 1998;95:7556–61.
2. Dunn GP, Bruce AT, Ikeda H, Old LJ, Schreiber RD. Cancer immunoediting: from immunosurveillance to tumor escape. Nat Immunol 2002;3:991–8.
3. Dunn GP, Bruce AT, Sheehan KC, Shankaran V, Uppaluri R, Bui JD, et al. A critical function for type I interferons in cancer immunoediting. Nat Immunol 2005;6:722–9.
4. Lesinski GB, Kondadasula SV, Crespin T, Shen L, Kendra K, Walker M, et al. Multiparametric flow cytometric analysis of inter-patient variation in STAT1 phosphorylation following interferon Alfa immunotherapy. J Natl Cancer Inst 2004;96:1331–42.
5. Critchley-Thorne RJ, Simons DL, Yan L, Miyahira AK, Dirbas FM, Johnson DL, et al. Impaired interferon signaling is a common immune defect in human cancer. Proc Natl Acad Sci U S A 2009;106:9010–5.
6. Gabrilovich DI, Nagaraj S. Myeloid-derived suppressor cells as regulators of the immune system. Nat Rev Immunol 2009;9:162–74.
7. Ostrand-Rosenberg S, Sinha P. Myeloid-derived suppressor cells: linking inflammation and cancer. J Immunol 2009;182:4499–506.
8. Gallina G, Dolcetti L, Serafini P, De Santo C, Marigo I, Colombo MP, et al. Tumors induce a subset of inflammatory monocytes with immunosuppressive activity on CD8+ T cells. J Clin Invest 2006;116:2777–90.
9. Bronte V, Wang M, Overwijk WW, Surman DR, Pericle F, Rosenberg SA, et al. Apoptotic death of CD8+ T lymphocytes after immunization: induction of a suppressive population of Mac-1+/Gr-1 +cells. J Immunol 1998;161:5313–20.
10. Corzo CA, Cotter MJ, Cheng P, Cheng F, Kusmartsev S, Sotomayor E, et al. Mechanism regulating reactive oxygen species in tumor-induced myeloid-derived suppressor cells. J Immunol 2009;182:5693–701.
11. Bronte V, Apolloni E, Cabrelle A, Ronca R, Serafini P, Zamboni P, et al. Identification of a CD11b(+)/Gr-1(+)/CD31(+) myeloid progenitor capable of activating or suppressing CD8(+) T cells. Blood 2000;96:3838–46.
12. Watanabe S, Deguchi K, Zheng R, Tamai H, Wang LX, Cohen PA, et al. Tumor-induced CD11b+Gr-1+ myeloid cells suppress T cell sensitization in tumor-draining lymph nodes. J Immunol 2008;181:3291–300.
13. Nagaraj S, Gabrilovich DI. Tumor escape mechanism governed by myeloid-derived suppressor cells. Cancer Res 2008;68:2561–63.
14. Nagaraj S, Schrum AG, Cho HI, Celis E, Gabrilovich DI. Mechanism of T cell tolerance induced by myeloid-derived suppressor cells. J Immunol 2010;184:3106–16.
15. Srivastava MK, Sinha P, Clements VK, Rodriguez P, Ostrand-Rosenberg S. Myeloid-derived suppressor cells inhibit T-cell activation by depleting cystine and cysteine. Cancer Res 2010;70:68–77.
16. Strassmann G, Jacob CO, Evans R, Beall D, Fong M. Mechanisms of experimental cancer cachexia. Interaction between mononuclear phagocytes and colon-26 carcinoma and its relevance to IL-6-mediated cancer cachexia. J Immunol 1992;148:3674–8.
17. Lesinski GB, Trefry J, Brasdovich M, Kondadasula SV, Sackey K, Zimmerer JM, et al. Melanoma cells exhibit variable signal transducer and activator of transcription 1 phosphorylation and a reduced response to IFN-alpha compared with immune effector cells. Clin Cancer Res 2007;13:5010–19.
18. Zimmerer JM, Lesinski GB, Kondadasula SV, Karpa VI, Lehman A, Raychaudhury A, et al. IFN-alpha-induced signal transduction, gene expression, and antitumor activity of immune effector cells are negatively regulated by suppressor of cytokine signaling proteins. J Immunol 2007;178:4832–45.
19. Lesinski GB, Anghelina M, Zimmerer J, Bakalakos T, Badgwell B, Parihar R, et al. The antitumor effects of IFN-alpha are abrogated in a STAT1-deficient mouse. J Clin Invest 2003;112:170–80.
20. Bunt SK, Yang L, Sinha P, Clements VK, Leips J, Ostrand-Rosenberg S. Reduced inflammation in the tumor microenvironment delays the accumulation of myeloid-derived suppressor cells and limits tumor progression. Cancer Res 2007;67:10019–26.
21. Le HK, Graham L, Cha E, Morales JK, Manjili MH, Bear HD. Gemcitabine directly inhibits myeloid derived suppressor cells in BALB/c mice bearing 4T1 mammary carcinoma and augments expansion of T cells from tumor-bearing mice. Int Immunopharmacol 2009;9:900–9.
22. Suzuki E, Kapoor V, Jassar AS, Kaiser LR, Albelda SM. Gemcitabine selectively eliminates splenic Gr-1+/CD11b +myeloid suppressor cells in tumor-bearing animals and enhances antitumor immune activity. Clin Cancer Res 2005;11:6713–21.
23. Jaime-Ramirez AC, Mundy-Bosse BL, Kondadasula S, Jones NB, Roda JM, Mani A, et al. IL-12 enhances the antitumor actions of trastuzumab via NK cell IFN-gamma production. J Immunol 2010;186:3401–09.
24. Dunn GP, Koebel CM, Schreiber RD. Interferons, immunity and cancer immunoediting. Nat Rev Immunol 2006;6:836–48.
25. Capuano G, Rigamonti N, Grioni M, Freschi M, Bellone M. Modulators of arginine metabolism support cancer immunosurveillance. BMC Immunol 2009;10:1.
26. Ko HJ, Kim YJ, Kim YS, Chang WS, Ko SY, Chang SY, et al. A combination of chemoimmunotherapies can efficiently break self-tolerance and induce antitumor immunity in a tolerogenic murine tumor model. Cancer Res 2007;67:7477–86.
27. Mazzoni A, Bronte V, Visintin A, Spitzer JH, Apolloni E, Serafini P, et al. Myeloid suppressor lines inhibit T cell responses by an NO-dependent mechanism. J Immunol 2002;168:689–95.
28. Brito C, Naviliat M, Tiscornia AC, Vuillier F, Gualco G, Dighiero G, et al. Peroxynitrite inhibits T lymphocyte activation and proliferation by promoting impairment of tyrosine phosphorylation and peroxynitrite-driven apoptotic death. J Immunol 1999;162:3356–66.
29. Llovera M, Pearson JD, Moreno C, Riveros-Moreno V. Impaired response to interferon-gamma in activated macrophages due to tyrosine nitration of STAT1 by endogenous nitric oxide. Br J Pharmacol 2001;132:419–26.
30. Sinha P, Clements VK, Ostrand-Rosenberg S. Reduction of myeloid-derived suppressor cells and induction of M1 macrophages facilitate the rejection of established metastatic disease. J Immunol 2005;174:636–45.
31. Ochoa AC, Zea AH, Hernandez C, Rodriguez PC. Arginase, prostaglandins, and myeloid-derived suppressor cells in renal cell carcinoma. Clin Cancer Res 2007;13:721s–6s.

32. Rodriguez PC, Ernstoff MS, Hernandez C, Atkins M, Zabaleta J, Sierra R, et al. Arginase I-producing myeloid-derived suppressor cells in renal cell carcinoma are a subpopulation of activated granulocytes. Cancer Res 2009;69:1553–60.
33. Rodriguez PC, Ochoa AC. Arginine regulation by myeloid derived suppressor cells and tolerance in cancer: mechanisms and therapeutic perspectives. Immunol Rev 2008;222:180–91.
34. Bronte V, Zanovello P. Regulation of immune responses by L-arginine metabolism. Nat Rev Immunol 2005;5:641–54.
35. Eisenbeis CF, Lesinski GB, Anghelina M, Parihar R , Valentino D, Liu J, et al. Phase I study of the sequential combination of interleukin-12 and interferon alfa-2b in advanced cancer: evidence for modulation of interferon signaling pathways by interleukin-12. J Clin Oncol 2005;23:8835–44.
36. Belardelli F, Ferrantini M, Proietti E, Kirkwood JM. Interferon-alpha in tumor immunity and immunotherapy. Cytokine Growth Factor Rev 2002;13:119–34.
37. Davis ID, Brady B, Kefford RF, Millward M, Cebon J, Skrumsager BK, et al. Clinical and biological efficacy of recombinant human interleukin-21 in patients with stage IV malignant melanoma without prior treatment: a phase IIa trial. Clin Cancer Res 2009;15:2123–9.
38. Motohashi S, Nagato K, Kunii N, Yamamoto H, Yamasaki K, Okita K, et al. A phase I-II study of alpha-galactosylceramide-pulsed IL-2/GM-CSF-cultured peripheral blood mononuclear cells in patients with advanced and recurrent non-small cell lung cancer. J Immunol 2009;182:2492–501.
39. Murad YM, Clay TM, Lyerly HK, Morse MA. CPG-7909 (PF-3512676, ProMune): toll-like receptor-9 agonist in cancer therapy. Expert Opin Biol Ther 2007;7:1257–66.
40. Critchley-Thorne RJ, Yan N, Nacu S, Weber J, Holmes SP, Lee PP. Down-regulation of the interferon signaling pathway in T lymphocytes from patients with metastatic melanoma. PLoS Med 2007;4:e176.